

Effects of the depth to coral height ratio on drag coefficients for unidirectional flow over coral

C. B. McDonald, J. R. Koseff,¹ and S. G. Monismith

Environmental Fluid Mechanics Laboratory, Department of Civil and Environmental Engineering, Stanford University, Stanford, California 94305-4020

Abstract

We investigated the effects of the ratio of water depth (H) to coral height (h) on the drag coefficient (C_d) for unidirectional flow over the coral species *Porites compressa*. C_d measured in a laboratory flume at several different flow rates and depths over a coral canopy, varied from 0 to 1.68 with a clear dependence on $H:h$. At higher Reynolds numbers C_d was inversely proportional to $H:h$ and showed signs of becoming Re-independent. C_d was dependent on both Re and $H:h$ at lower Reynolds numbers, indicating laminar or transitional flow within the coral canopy. The relationship between C_d and $H:h$ at the highest available Re for each depth ratio is described by the power law: $C_d = 1.01(H:h)^{-2.77} + 0.01$. This result should be applied with caution, however, as different coral species and bottom roughness may cause a deviation from this relationship.

Introduction

Coral reefs are among the most productive ecosystems in the world despite being generally located in oligotrophic ocean regions (Hatcher 1988, 1990). For many years the prevailing view was that efficient recycling of nutrients as a result of tight coupling between reef organisms was responsible for this anomalously high production (Hatcher 1990). More recently, however, it has become clear that many natural reef systems are mass transfer–limited (Bilger and Atkinson 1995; Baird and Atkinson 1997; Thomas and Atkinson 1997), i.e., the supply of nutrients to facilitate reef growth is affected by the thickness of the diffusive boundary layer (DBL), across which diffusion of nutrients must occur down a concentration gradient before they can be assimilated by reef organisms. Given that the thickness of the DBL decreases with increasing velocity shear at the coral surface (Hearn et al. 2001), higher mass transfer and therefore nutrient flux rates are expected where velocities are higher. Thus, as originally suggested by Munk and Sargent (1954), the reason reefs are most productive at their margins is because water velocities (often because of surface waves) are generally higher there than in more protected inshore regions.

Coral reefs are far more geometrically complex than the kinds of roughness generally found in engineering flows (Kaandorp and Kuebler 2001); nonetheless, DBL thickness, turbulence production, and mass transfer are correlated with

the drag force on flows moving over the reef (Atkinson and Bilger 1992; Atkinson et al. 2001; Falter et al. 2004). The total drag on the reef, which is the combination of the form drag resulting from the general shape of the coral roughness elements, and skin friction because of flow around and through the coral, can be parameterized in terms of a drag coefficient C_d . C_d is thus dependent on the morphology and density of coral cover (roughness), and flow characteristics such as water velocity and depth (Thomas and Atkinson 1997). In fact, as shown briefly by Hearn et al. (2001), C_d should scale with the ratio of roughness length (traditionally the height above the bottom where flow velocity is zero) to total depth.

In this study we investigate the relationship between the ratio of water depth (H) to the maximum coral height (h) and C_d for unidirectional flow over a coral surface of *Porites compressa*. The effect of this depth ratio on drag has been relatively well studied in unconfined canopy flow (e.g., Coceal and Belcher 2004; Raupach et al. 1996) and vegetative canopies (e.g., Nepf and Vivoni 2000) where the roughness elements may emerge out of the flow. However, relatively few studies in the literature have reported values of C_d for flow over coral (Baird and Atkinson 1997; Thomas and Atkinson 1997; Reidenbach 2004). Furthermore, these reported values vary from 0.01 (Reidenbach 2004) to almost 0.3 (Thomas and Atkinson 1997). The purpose of the present study is to attempt to reconcile this large variation in reported C_d values based on this “depth ratio” scaling parameter and its effect for unidirectional flow. In order to do this, we performed a series of laboratory flume experiments with unidirectional flow over a coral pavement made up of *Porites compressa* skeletons. As described below, we measured C_d for a variety of flow velocities and depth ratios ($H:h$).

Methods

Laboratory experiments were conducted in a 10-m-long by 0.6-m-wide recirculating flume in which flow was driven over a coral pavement of length 2.8 m (L) with a maximum height of 18 cm (h) (see Fig. 1A,B). A steady, unidirectional

¹ Corresponding author.

Acknowledgments

We thank Bob Brown for his design and building expertise. We also thank Ryan Lowe, Matt Reidenbach, and Cary Troy for their assistance in the lab and helpful discussions. Funding for C.B.M. was provided in part by the generous support of a Bright Futures Fellowship from the New Zealand Foundation for Research, Science, and Technology (FRST) and from the National Science Foundation under grant number OCE 0117859. We would also like to thank the two anonymous reviewers whose comments and suggestions contributed significantly to the final manuscript.

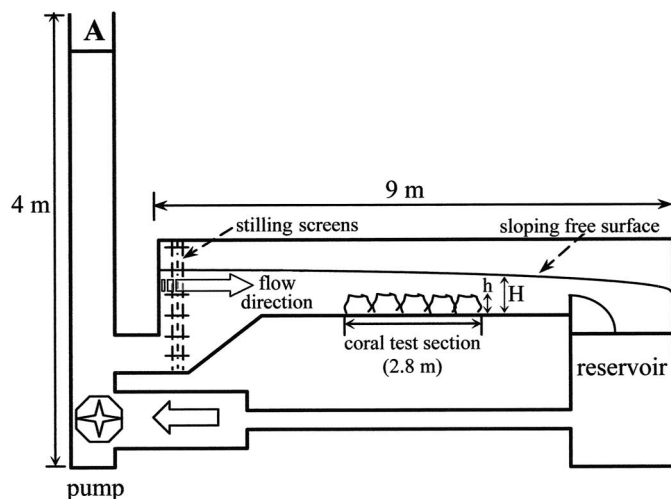


Fig. 1. (A) Schematic diagram of laboratory flume setup. (B) Photo of flume with ADV setup visible.

flow of depth H (measured from the flume bottom to the free surface at the end of the test section) was generated by a constant-head tank and controlled downstream by a sharp-crested weir. For the five different depth ratios ($H:h$), obtained by varying the flow depth from 20 to 40 cm in 5-cm increments, flow rates were adjusted using combinations of pump settings and weir heights. For a full description of the flume, see O'Riordan et al. (1993). The coral canopy comprised actual coral heads (*Porites compressa*) arranged over the entire width of the flume, such that the largest heads were in the middle of the 2.8-m test section in order to re-

duce recirculation zones in the wakes of the coral heads. This arrangement closely resembled a natural *Porites compressa* canopy (see fig. 1 in Lowe et al. 2005); furthermore, slight variations to this arrangement had no effect on the pressure drop, as evidenced by the fact that the pressure drop did not vary even though the corals were taken in and out of the flume several times during these experiments.

In the present experiments, the pressure gradient, provided by the free surface slope (S), balances the bottom stress because of the coral and the shear stress from the flume walls. The sidewall stress is negligible but can be accounted for by subtracting the pressure drop measured for each flow case without coral from the pressure drop measured for flow with the coral elements present. The resulting force balance can be shown to determine C_d in terms of the overall flow depth H , bulk flow velocity U_b , g , and S (Bilger and Atkinson 1992; Baird and Atkinson 1997):

$$C_d = \frac{2gHS}{U_b^2} \quad (1)$$

In addition to ($H:h$), C_d is also dependent on the Reynolds number (Re ; the ratio of inertial forces to viscous forces), which is defined for each flow in this experiment as:

$$Re = \frac{U_b R_h}{\nu} \quad (2)$$

where R_h is the hydraulic radius (cross-sectional area divided by wetted perimeter), and ν is the kinematic viscosity ($9.8 \times 10^{-7} \text{ m}^2 \text{ s}^{-1}$). It should be noted that in the previous flume studies that have measured C_d over coral (e.g., Baird and Atkinson 1997), Re was defined as $Re = 4HU_b/\nu$ in order to facilitate comparison of measured parameters with those reported in the engineering literature for equivalent pipe flows. In this study, however, the hydraulic radius and true bulk velocity were chosen, because they are the length and velocity scales typically used in the engineering literature for open channel flows. Furthermore, the shear layer of varying strength at the top of the canopy (because of coral drag) means that bulk velocity within the canopy is retarded, and bulk velocity above the canopy is accelerated. The magnitude of these effects is a nonlinear function of the flow rate (see Table 1). The most appropriate velocity scale for Re to best characterize the overall flow conditions is thus the overall bulk velocity, which accounts somewhat for these shear layer effects.

The free surface slope S was computed by measuring the pressure drop over the coral pavement using a Validyne DP-15 variable reluctance pressure sensor (full range = ± 8 cm water). The sensor was connected by plastic tubing to the bottom of the flume at the beginning and end of the coral section. The sensitivity of the sensor to its orientation and that of the plastic tubing was the main source of uncertainty in the pressure measurement. This was minimized by keeping the tubing in a constant, fixed position for the calibration and subsequent measurements; additionally, the zero was regularly checked in a still flume, and the sensor recalibrated frequently. The sensor was calibrated using a custom device consisting of two interconnected measuring cylinders attached to each side of the pressure sensor by plastic tubing.

Table 1. A summary of measured and calculated parameters for each flow; see text for the definition of each.

H (m)	ΔP (m)	$(H:h)$	Re	Re within coral canopy	U_b (cm s ⁻¹)	U_b within coral canopy	C_d	Surface velocity (cm s ⁻¹)
0.201	0.0010	1.11	4,015	570	3.3	1.4	1.31	6.6/11.5*
0.198	0.0064	1.10	8,955	1,130	7.4	2.7	1.68	16.9/26.7
0.203	0.0109	1.12	14,075	2,220	11.4	5.4	1.22	21.1/35.9
0.203	0.0201	1.12	23,960	4,745	19.4	11.5	0.78	29.9/47.9
0.201	0.0308	1.11	29,470	5,410	24.0	13.1	0.77	41.1/58.7
0.253	0.0002	1.40	4,827	330	3.5	0.8	0.32	8.8
0.251	0.0020	1.39	10,920	1,030	7.8	2.5	0.57	18.4
0.248	0.0058	1.37	18,590	2,290	13.4	5.5	0.57	30.5
0.248	0.0107	1.37	28,340	4,415	20.5	10.7	0.45	40.1
0.247	0.0169	1.37	37,560	6,315	27.2	15.2	0.41	49.8
0.300	0.0001	1.66	6,750	250	4.4	0.6	0.15	10.2
0.301	0.0013	1.66	14,820	1,160	9.7	2.8	0.30	20.1
0.302	0.0032	1.66	27,410	4,060	17.9	9.8	0.22	30.0
0.302	0.0060	1.66	38,820	6,485	25.3	15.7	0.20	39.8
0.303	0.0099	1.67	51,850	9,550	33.7	23.0	0.19	49.7
0.352	0.0000	1.95	8,590	495	5.2	1.2	0.00	10.1
0.351	0.0010	1.94	18,730	1,995	11.3	4.8	0.19	19.7
0.347	0.0027	1.92	31,180	4,260	19.0	10.3	0.19	30.5
0.348	0.0046	1.93	41,970	6,680	25.5	16.1	0.17	39.3
0.348	0.0080	1.93	58,790	10,685	35.8	25.2	0.16	50.0
0.398	0.0000	2.20	9,870	370	5.6	0.9	0.00	10.1
0.402	0.0007	2.22	21,800	1,920	12.4	4.6	0.13	20.0
0.401	0.0020	2.22	35,620	4,385	20.3	10.6	0.14	30.4
0.401	0.0038	2.22	50,240	8,390	28.7	20.3	0.13	39.7

* For the shallowest depth only, ADV measurements of surface velocity were taken both directly over a coral head, and over a gap or channel. Both measurements are shown above respectively.

By draining one cylinder relative to the other in precisely determined increments, the linear relationship between voltage and surface elevation is obtained.

The bulk flow rate (in $\text{m}^3 \text{s}^{-1}$) was obtained from the weir equation (French 1985):

$$Q = \frac{2}{3} C_e h_1 W \sqrt{2gh_1} \quad (3)$$

where h_1 is the vertical distance from the weir to the water surface measured at the point where the water surface begins to slope, $C_e = 0.602 + 0.075h_1/P$, W is the width of the flume (0.6 m), and P is the weir height in meters. The bulk velocity (U_b) was then calculated by dividing the bulk flow rate by the cross-sectional area of the flow, $A = HW$.

Velocities above the coral pavement were measured using a Sontek Acoustic Doppler Velocimeter (ADV) sampling at 10 Hz. These measurements, along with measurements of canopy height, were used to estimate the total flow above the canopy in each case. The flow rate through the canopy could then be determined by subtracting this estimate from the bulk flow rate Q .

There were no significant transverse or streamwise variations in along-flume velocities for the three deepest flows ($H = 30, 35,$ and 40 cm); thus, in these cases, the above-canopy flow was calculated from the cross-sectional area above the coral, and a vertical velocity profile measured in the middle of the test section. In contrast, for $H = 25$ cm, there were streamwise velocity variations, and the shallowest flow ($H = 20$ cm) showed both transverse and streamwise variations. For $H = 25$ cm, the test section was divided into longitudinal sections and velocities measured in each section. These velocities, together with the height of water above the coral, were used to calculate a flow rate per unit width for each section. Above-canopy flow was then calculated by multiplying a weighted average of these sectional two-dimensional flow rates by the flume width. In the shallowest case ($H = 20$ cm), the transverse variation was present only in the middle section—reflecting whether the velocity was measured above a channel or a coral head (see Table 1). Thus, for $H = 20$ cm, the flow rate per unit width for this central test section was calculated taking this variation into account, and the overall above-canopy flow then calculated as for the $H = 25$ cm case.

Results

The depth ratio ($H:h$) was varied from 1.1 to 2.2 by manipulating the pump setting and weir height to alter the flowing depth (H). Table 1 shows the results for several different flow rates at each depth ratio. The drag coefficients (C_d) and Re were calculated from the measured data using Eq. 1 and Eq. 2 respectively. The bulk velocity within the canopy was determined by estimating the fraction of bulk flow passing through the coral canopy as described in the methods section above, then dividing this flow rate by the canopy cross-sectional area (based on maximum coral height h , and flume width W). The Reynolds number for this canopy flow was calculated using the hydraulic radius of the portion of the

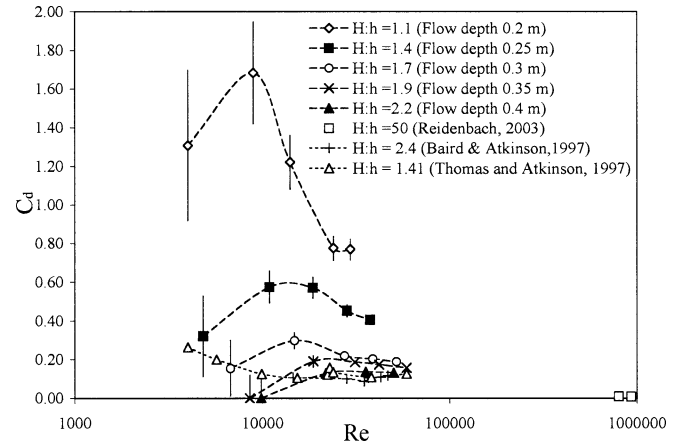


Fig. 2. Plot of C_d versus Reynolds number for different values of $H:h$. Included is each flow from this study and all other available data (Baird and Atkinson 1997; Thomas and Atkinson 1997; Reidenbach 2004). Error bars are shown only where they exceed the size of the point. Note that the data from Thomas and Atkinson (1997) and Baird and Atkinson (1997) are not directly comparable because of differences in the way bulk velocity was measured; see text for further explanation.

flume occupied by the coral canopy as the appropriate length scale.

As shown in Table 1, the pressure drop over the coral section increased both as velocity increased and depth ratio decreased. As a result, calculated drag coefficients generally increased as the depth ratio decreased towards 1 (the limit where the coral occupies the entire water column)—showing a marked increase for the lowest $H:h$ (1.11). The bulk Reynolds numbers in this experiment ranged from 4,000 to 59,000, whereas the Reynolds numbers estimated for flow within the canopy were much lower (ranging from 238 to 10,700), suggesting the possibility of laminar or transitional flow within the canopy for many of the lower flow rates. The bulk velocities ranged from 3.3 to 35.8 cm s^{-1} ; these were significantly lower in all cases than the near-surface velocities (U_s) measured above the coral by ADV, which were around 10–12 cm s^{-1} for the lowest flow rates and as high as 50 cm s^{-1} for the highest (see Table 1). Additionally, the relationship between bulk velocity and surface velocity was variable, with the ratio of U_b to U_s tending to increase as flow rate increased for a given $H:h$. This suggests that as flow rate was increased relatively more fluid was forced to go through the canopy region.

Plots of C_d versus Re for each $H:h$ are presented in Fig. 2. Each curve represents the trend in C_d for a fixed $H:h$ as the Reynolds number of the flow increases. The curves clearly show the general trend of decreasing C_d with increasing $H:h$ at a given Re ; also evident in each curve is a characteristic “convex hump” at the lower Reynolds numbers followed by a sharp decrease in C_d at higher Re , and then a leveling out as Re continues to increase. This low Reynolds number feature may be because of the apparent laminar-turbulent transition occurring within the canopy, as shown by the Re values estimated for the subcanopy layer in Table 1. Also included in Fig. 2 are the only other lab data available for *Porites compressa* (Baird and Atkinson 1997; Thomas

and Atkinson 1997), with their Reynolds number recalculated according to the definition used in this study for comparison, and two points from a field experiment conducted over a reef in Eilat, Israel (Reidenbach 2004).

The Baird and Atkinson (1997) and Thomas and Atkinson (1997) data are generally similar to those presented from this experiment but do not show the “hump” at low Reynolds number discussed above. It should be noted, however, that their bulk velocity was measured by a surface float and thus is more representative of U_s , which, as seen in our ADV measurements, is significantly greater than the bulk velocity (Table 1). When this is factored in these two sets of data points would tend to move up (towards higher C_d) and to the left (towards lower Re) with the upward shift being larger (as C_d is inversely proportional to U_b^2 , and Re is only proportional to U_b). The relationship between surface and bulk velocity is Re-dependent, with bulk velocity becoming a larger fraction of the surface velocity as Re increases for a given $H:h$; this means that the points at lower Re would shift even further up for each curve. Thus, if the velocities were equivalent, it is quite possible that the low Re feature would be present for both sets of data. Furthermore, the $H:h = 1.41$ data of Thomas and Atkinson (1997) could move upward towards higher C_d , achieving better agreement with the $H:h = 1.4$ curve from this study. The points of Reidenbach (2004) were measured in the field in 10 m of water where the coral roughness was around 20 cm, and thus $H:h$ was approximately 50. These data represent the highest available $H:h$ for C_d over corals that has been measured.

The main contributions to uncertainty in the calculation of C_d are the errors in the pressure measurement and in the measurement of the height h_1 . The pressure sensor is somewhat sensitive to motion of the plastic tubing connecting it with the tank, meaning that small pressure drops for the lowest flow rates are hard to distinguish from this external variability. The parameter, h_1 , is measured at a variable distance from the weir at the point where the water surface begins to slope down to pass over the weir; this is more difficult to discern and measure for the low flow cases. These difficulties result in the greater uncertainty observed in calculated values of C_d both for lower Re and for lower depth at a given Re (the reduced uncertainty from a larger pressure drop is more than compensated for by the larger uncertainty in h_1 as depth decreases). The uncertainty in C_d is not significant for many of the higher Re points (less than the size of the point in Fig. 2).

The relationship between C_d and $H:h$ at the highest Re for each experiment is presented in Fig. 3. Fig. 3 shows C_d from this study, and the available high-Re limit points from the Reidenbach field study, as a function of $H:h$ (on a log scale) for the high-Re (flatter) part of the curve. Also shown in Fig. 3 are all the available data from Thomas and Atkinson (1997) and Baird and Atkinson (1997), and the best-fit power law line (using only data from this experiment and Reidenbach 2004). Again, it is important to note that the data points from these two laboratory flume studies at lower Re would shift up (low Re points relatively more) if C_d was calculated with true bulk velocity, and would likely agree better with the best-fit curve. For this reason, and because many of these data are from species other than *Porites com-*

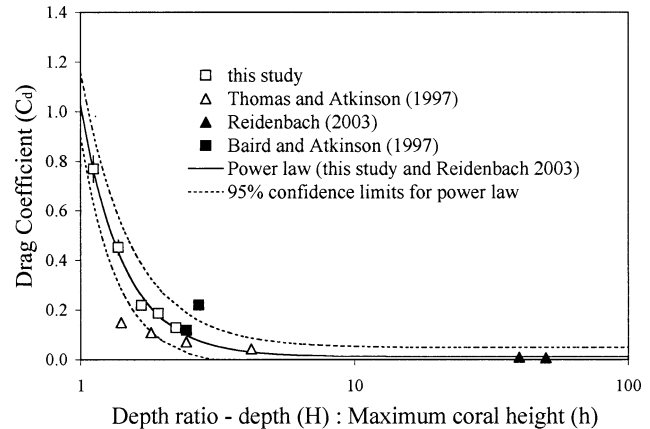


Fig. 3. Plot of C_d versus $H:h$ at the highest Re available for each $H:h$. The best-fit power law ($C_d = 1.01(H:h)^{-2.77} + 0.01$) is displayed (solid line) along with curves representing the 95% confidence interval for the coefficients (dotted lines). These curves only include data from this study and Reidenbach (2003). All other available data are plotted for comparison but omitted from the best-fit calculations because of differences in the velocity measurements (as described in the text).

pressa, these points are included on the plot but omitted from the best-fit calculations.

The best-fit power law in Fig. 3 ($C_d = 1.01(H:h)^{-2.77} + 0.01$) suggests C_d scales with $(H:h)^{-2.77}$ and asymptotes to a value of 0.01 at large values of $H:h$. As $H:h$ approaches 1, there is an increasingly greater influence on C_d with the effect becoming much less significant for $H:h > 2$. C_d is predicted to be around 0.2 in the vicinity of $H:h = 2$ (Fig. 3). This is consistent with depth ratios found in studies that have previously measured values of C_d over coral (e.g., Baird and Atkinson 1997; Thomas and Atkinson 1997), especially given the differences in velocity measurements described above. The best-fit asymptotic value of 0.01 at high $H:h$ is driven by the points of Reidenbach (2004) and may represent the high $H:h$ limit for C_d over coral. There is no available data in the intervening range of $H:h$, and unfortunately we were unable to obtain data in this range with the flume setup in this experiment.

Discussion

In this experiment, C_d calculated for unidirectional flow over coral is clearly dependent on $H:h$ and Re over the lower range of Reynolds numbers, but we see evidence of C_d becoming independent of Re (C_d vs. Re curves appear to flatten out for every $H:h$) as Re increases. Similar behavior is observed for traditional engineering flows, e.g., flow in pipes, for which, above a certain Reynolds number, the friction factor depends only on the relative roughness as the flow becomes “fully rough” (represented by the Moody diagram).

The low Reynolds number “convex hump” effects on drag coefficient observed in Fig. 2 are also analogous to well-studied flows in the engineering literature. For example, similar features are observed in plots of C_d versus Re for flow over a flat plate (e.g., fig. 10.10 in Kundu and Cohen

2002) and in pipe flow (i.e., the Moody diagram) as the transition from laminar to turbulent flow occurs. In such engineering studies, C_d for laminar flow is high, decreasing as Re increases until the flow is tripped into turbulence—initially causing an increase in C_d and then, as Re continues to increase, a rapid decay in C_d as the flow becomes fully turbulent. The similarity of these results to the C_d versus Re curves in this study, along with the Re 's calculated for the within-canopy flow (Table 1) strongly suggests that we observe a transitional region at the lower end of Re values achieved in this study, as well as a fully turbulent regime at higher values of Re .

Where flow over coral (as in this study) begins to differ dramatically from typical engineering flows is in the magnitude of the drag coefficient. This also has an effect on mass transfer rates, which are higher than expected from established engineering equations for similar roughness heights (Atkinson and Bilger 1992; Bilger and Atkinson 1992). Using a scaling approach based on the log law for rough boundary layer flows (see Kundu and Cohen 2002, pp. 534–535), Hearn et al. (2001) conclude that “the only way of achieving such high drag coefficients is for the roughness length to be an appreciable fraction of the water depth.” Their analysis estimates that, in order to achieve a value of C_d around 100 times that of a sandy bottom (~ 0.0025), the depth should be approximately twice the roughness length (i.e., $H:h \sim 2$).

In this approach however, the value of $H:h$ for a sandy bottom where C_d is relatively well known is assumed to be 200. In reality, for a sand roughness length on the order of a few millimeters, $H:h$ can vary by orders of magnitude depending on the depth. Furthermore, although the result of Hearn et al. was ostensibly consistent with previous measurements for flow over coral (Baird and Atkinson 1997; Thomas and Atkinson 1997; Lugo-Fernandez et al. 1998), as $H:h$ approaches 1, the C_d predicted by the Hearn et al. (2001) scaling analysis is significantly different to that found in this study (e.g., see Fig. 3).

Clearly, corals are different from typical roughness elements in that there is significant flow through the roughness, and the roughness can occupy a very large fraction of the water column (the entire water column if $H:h = 1$). It seems unlikely that the log law will hold under these conditions, and consequently these features of coral canopies are the likely cause of the difference between the result of Hearn et al. (2001) and the relationship between C_d and $H:h$ in this study.

Figure 4 presents C_d as a function of the estimated percentage of flow diverted up and over the coral canopy that would have flowed through the region occupied by the coral if there had been no corals in the flume. The percentage of flow through the canopy region in the absence of corals was calculated for each flow rate by integrating a typical approximation to the velocity profile for an open channel:

$$U(z) = U_0 \left(\frac{z}{H} \right)^{1/7} \quad (4)$$

where U_0 , the free stream velocity, is assumed to be $8/7U_b$, and z is the vertical coordinate. The percentage of flow

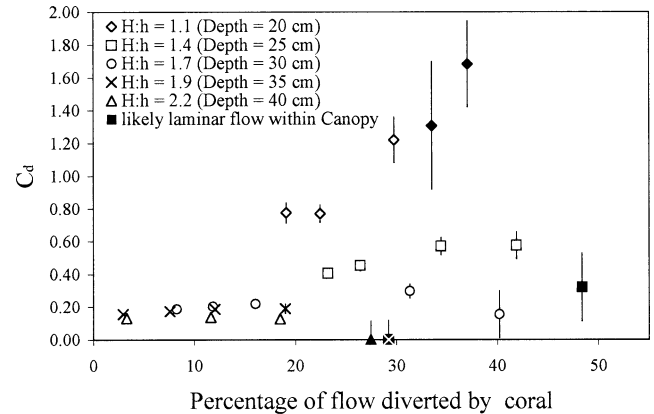


Fig. 4. Plot of C_d versus percentage of flow diverted by the coral canopy. This shows the effect on C_d of the fluid volume exchanged with the overlying water column (expressed as percentage of flow diverted; see text for explanation of how this was calculated). For a given percentage diverted, the relative volume (and thus impact on C_d) of fluid exchanged from within the canopy is greater as $H:h$ decreases.

through the canopy region in the presence of corals was obtained by calculating the flow above the canopy using the ADV measurements and subtracting this from the calculated flow rate. ADV measurements immediately above the coral for the shallowest case ($H = 20$ cm) included the velocity directly above a coral head and the velocity between coral heads, i.e., directly above a gap or channel. In all cases, the velocity above a channel was significantly greater than the velocity above a coral head, suggesting that the flow within the canopy was channelized with little flow through the coral heads themselves. Finally, the percentage of the total flow diverted by the presence of the coral canopy is simply the difference between the percentage of the flow through the canopy region calculated for the no-coral case and the percentage of flow through the corals estimated from ADV measurements.

Figure 4 shows that for each value of $H:h$, C_d increases as a greater percentage of the flow is diverted or exchanged into the zone above the canopy. The effect is more pronounced for $H:h$ approaching 1, with the slope of the curves of C_d versus percentage diverted consistently decreasing as $H:h$ gets larger, i.e., as the coral becomes a smaller fraction of the water column. For all depths except the shallowest case, the points for the lowest flow rates (generally also the highest percentage diverted) are not consistent with the trend of C_d increasing as more flow is diverted, although the errors associated with these points are much larger. The most likely reason for this is the sensitivity limit of the pressure sensor; when the flow was slow and/or deep, the pressure drop was recorded as zero or close to zero, thereby reducing the calculated C_d .

The main source of uncertainty in the computed percentage of the flow diverted is the calculation of the flow above the coral based on our ADV measurements. The exact velocity profile above the coral is not known, making it impossible to estimate the uncertainty in the percentage diverted. However, for each depth the same assumptions were

made in calculating the above-coral flow, meaning that the “percentage diverted” points will be accurately placed relative to each other. The fact that the exact amount of diverted flow is unknown is not important, because the conclusions and interpretations that follow are drawn based on the relative placement of these points.

The bulk velocity through the coral canopy is significantly lower in every instance than in the flow passing above the canopy (Table 1). Thus, the water that is exchanged into the region above the coral from within the canopy is of lower momentum than the water already passing through this region, and this lower-momentum fluid exerts drag on the water column above. This explanation accounts for the trends observed in Fig. 4: C_d increases as more low-momentum fluid is diverted from within the canopy (increased drag on the water column). The effect is much more pronounced as $H:h$ approaches 1 because the volume of lower-momentum fluid becomes a larger fraction of the flow above the coral. As $H:h$ becomes greater, the relative amount of lower-momentum fluid exchanged from within the canopy continues to decrease, and thus the correlation between C_d and the percentage of flow diverted weakens quickly. For $H:h$ greater than 2, the diverted fluid has a greatly reduced effect on C_d (Figs. 3, 4).

This explanation is similar to that offered in a different experiment for simulated flow over vegetation (Wu et al. 1999). They found an increase in Manning’s roughness coefficient (n), which is related to C_d in the region $1 < H:h < 1.5$ (their D/T), and attributed this to the greater influence of the boundary shear layer at the top of the canopy. As the relative height of the vegetation reduced (increasing $H:h$), the effect of this boundary shear became insignificant, as was found in this study for coral at approximately $H:h > 2$. In addition, for the submerged region of these vegetative flows Wu et al. obtained curves very similar in shape to Fig. 2 from this study (see figs. 2b and 4 in Wu et al. 1999), although the plotted parameters were slightly different (n vs. depth).

These results also exhibit parallels to the mixing-layer analogy for unconfined canopy flow (Raupach et al. 1996; Ghisalberti and Nepf 2002); essentially, the mixing-layer analogy represents the high $H:h$ limit. Flow in an unconfined canopy is analogous to the classic turbulent mixing layer (see Pope 2000), where two streams of different velocity initially separated by a splitter plate mix with an inflection point in the velocity profile at the level of the plate or top of the canopy. Above and below the mixing layer, the velocities are the free stream velocities of the respective layers. As $H:h$ decreases towards 1, the mixing layer becomes a significant fraction of the zone above the canopy, then occupying the entire above-canopy zone, increasingly influencing the momentum of this zone and consequently C_d .

The presence of the coral canopy causes relatively low-momentum fluid from within the canopy to be exchanged vertically with the higher-momentum water column above the canopy. The interaction of this slower-moving fluid (that would have otherwise flowed through the region occupied by the coral in the absence of the canopy) with the overlying water column causes increased drag on the water column above the coral, resulting in the observed higher than ex-

pected drag coefficients. As $H:h$ decreases towards its lower limit of 1, the amount of low-momentum fluid diverted into the above-canopy zone is an increasingly larger fraction of the total volume of fluid above the canopy, and thus has a proportionately greater effect on the momentum of the upper layer and C_d . That is, as $H:h$ decreases to 1, C_d increases rapidly because of the presence of relatively more low-momentum fluid from within the canopy. As Re increases for a given $H:h$ (i.e., increasing flow rate at a constant depth in this experiment), C_d decreases as more fluid is forced through the canopy, so a smaller fraction of the total flow is diverted into the upper layer. In the region $H:h > 1.9$, the volume of diverted fluid relative to the total volume of the overlying water column becomes increasingly insignificant, hence the reason C_d is less sensitive to $H:h$ in this region and corals begin to look more like traditional roughness elements at these values of $H:h$.

This finding has potentially important implications for both vertical and horizontal mass transfer in coral reef systems. In shallow reef environments, $H:h$ will change significantly over a tidal cycle and thus drag will be maximized either side of low tides. This would produce an asymmetry over a tidal cycle in nutrient cycling and sediment resuspension. It could also result in significant differences in currents between low and high tides, thus producing significant residual velocities that could be very important for advective transport in coral lagoons. Furthermore, coral mass transfer experiments in laboratory flumes should take into consideration the effect of $H:h$ on C_d when interpreting results.

Flow properties such as velocity and hydrodynamic drag have been shown to influence many aspects of coral ecology, including growth, energetics, morphology, nutrient uptake, and spatial distributions (e.g., Fabricius 1997; Atkinson et al. 2001; Genovese and Whitman 2004). The fact that the drag, as represented by C_d , is dependent on the depth ratio, $H:h$, suggests that this ratio may be an important factor to consider when interpreting the ecological effects of physical flow in shallow reef environments with predominantly unidirectional currents.

References

- ATKINSON, M. J., AND R. W. BILGER. 1992. Effects of water velocity on phosphate uptake in coral reef-flat communities. *Limnol. Oceanogr.* **37**: 273–279.
- ATKINSON, M. J., J. L. FALTER, AND C. J. HEARN. 2001. Nutrient dynamics in the Biosphere 2 coral reef mesocosm: Water velocity controls NH_4 and PO_4 uptake. *Coral Reefs* **20**: 341–346.
- BAIRD, M. E., AND M. J. ATKINSON. 1997. Measurement and prediction of mass transfer to experimental coral reef communities. *Limnol. Oceanogr.* **42**: 1685–1693.
- BILGER, R. W., AND M. J. ATKINSON. 1992. Anomalous mass transfer of phosphate on coral reef flats. *Limnol. Oceanogr.* **37**: 261–272.
- . 1995. Effects of nutrient loading on mass-transfer rates to a coral-reef community. *Limnol. Oceanogr.* **40**: 279–289.
- COCEAL, O., AND S. E. BELCHER. 2004. A canopy model of mean winds through urban areas. *Q. J. R. Meteorol. Soc.* **130**: 1349–1372.
- FABRICIUS, K. E. 1997. Soft coral abundance on the central Great Barrier Reef: Effects of *Acanthaster planci*, space availability,

- and aspects of the physical environment. *Coral Reefs* **16**: 159–167.
- FALTER, J. L., M. J. ATKINSON, AND M. A. MERRIFIELD. 2004. Mass-transfer limitation of nutrient uptake by a wave-dominated reef flat community. *Limnol. Oceanogr.* **49**: 1820–1831.
- FRENCH, R. H. 1985. *Open channel hydraulics*. McGraw-Hill.
- GENOVESE, S. J., AND J. D. WHITMAN. 2004. Wind-mediated diel variation in flow speed in a Jamaican back reef environment: Effects on ecological processes. *Bull. Mar. Sci.* **75**: 281–293.
- GHISALBERTI, M., AND H. M. NEPF. 2002. Mixing layers and coherent structures in vegetated aquatic flows. *J. Geophys. Res.* **107**: 3-1–3-11.
- HATCHER, B. G. 1988. Coral reef primary productivity a beggars banquet. *Trends Ecol. Evol.* **3**: 106–111.
- . 1990. Coral reef primary productivity a hierarchy of pattern and process. *Trends Ecol. Evol.* **5**: 149–155.
- HEARN, C. J., M. J. ATKINSON, AND J. L. FALTER. 2001. A physical derivation of nutrient-uptake rates in coral reefs: Effects of roughness and waves. *Coral Reefs* **20**: 347–356.
- KAANDORP, J. A., AND J. E. KUEBLER. 2001. *The algorithmic beauty of seaweeds, sponges and corals*, 1st ed. Springer-Verlag.
- KUNDU, P., AND I. COHEN. 2002. *Fluid mechanics*, 2nd ed. Academic Press.
- LOWE, R. J., J. R. KOSEFF, AND S. G. MONISMITH. 2005. Oscillatory flow through submerged canopies. Part 1. Velocity structure. *J. Geophys. Res.* **110**, C10016, [doi:10.1029/2004JC002788].
- LUGO-FERNANDEZ, A., H. H. ROBERTS, W. J. WISEMAN, AND B. L. CARTER. 1998. Water level and currents of tidal and infragravity periods at Tague Reef, St. Croix (USVI). *Coral Reefs* **17**: 343–349.
- MUNK, W., AND M. SARGENT. 1954. Adjustment of Bikini Atoll to ocean waves. p. 275–280. U.S. Geol. Surv. Prof. Paper 260.
- NEPF, H. M., AND E. R. VIVONI. 2000. Flow structure in depth-limited, vegetated flow. *J. Geophys. Res.* **105**: 28547–28557.
- O'RIORDAN, C. A., S. G. MONISMITH, AND J. R. KOSEFF. 1993. A study of concentration boundary-layer formation over a bed of model bivalves. *Limnol. Oceanogr.* **38**: 1712–1729.
- POPE, S. B. 2000. *Turbulent flows*. Cambridge University Press.
- RAUPACH, M. R., J. J. FINNIGAN, AND Y. BRUNET. 1996. Coherent eddies and turbulence in vegetation canopies: The mixing-layer analogy. *Boundary-Layer Meteorol.* **78**: 351–382.
- REIDENBACH, M. 2004. *Boundary layer dynamics in coral reef systems*. PhD. thesis. Stanford Univ.
- THOMAS, F. I. M., AND M. J. ATKINSON. 1997. Ammonium uptake by coral reefs: Effects of water velocity and surface roughness on mass transfer. *Limnol. Oceanogr.* **42**: 81–88.
- WU, F. C., H. W. SHEN, AND Y. J. CHOU. 1999. Variation of roughness coefficients for unsubmerged and submerged vegetation. *J. Hydraul. Eng.* **125**: 934–942.

Received: 31 March 2005

Accepted: 3 October 2005

Amended: 4 November 2005